CHOCO-JEX: A Research Experiment Focused on the CHOCO Low-level Jet over the Far Eastern Pacific and Western Colombia

Johanna Yepes[1], Germán Poveda[1], John F. Mejía[2], Leonardo Moreno[3], Carolina Rueda[4]

[1]Universidad Nacional de Colombia, Sede Medellín, Facultad de Minas, Departamento de Geociencias y Medio Ambiente, Medellín, Colombia

[2] Department of Atmospheric Sciences/Desert Research Institute, Reno, NV, United States

[3] Dirección General Marítima, Bogotá, Colombia

[4]Subdirección de Meteorología, Fuerza Aérea Colombiana, Bogotá, Colombia

Capsule:

Scientists and students from Colombia and the United States, in cooperation with the Air Force and the General Maritime Directorate of Colombia, participated in CHOCO-JEX, the first field campaign to provide upper-air observations over the far eastern Pacific and western Colombia, a region that has one of the rainiest spots on Earth.

Correspondence to:

Germán Poveda, Department of Geosciences and Environment, Universidad Nacional de Colombia, Medellín, Colombia. gpoveda@unal.edu.co

Abstract

CHOCO-JEX experiment is an inter-institutional research program developed by the Universidad Nacional de Colombia, the General Maritime Directorate of the Ministry of National Defense of Colombia, the Colombian Air Force, and the Desert Research Institute at Reno, Nevada, US. The main goal of CHOCO-JEX is to characterize the vertical structure of the low-level Choco jet (ChocoJet) through observations and modeling. Thus, four 7-day Intensive Observation Periods (IOP) took place in different seasons in 2016, two over land and two over the far eastern Pacific off the coast of Colombia, including the deployment of upper-air soundings 4 times per day to monitor the predominant diurnal cycle and the synoptic and seasonal variability. Preliminary results show deeper westerly moisture flow and strong diurnal cycle over land than over ocean. IOP4 provides the first observational evidence of the southwesterly ChocoJet with mean winds of 5 m/s. Diurnal cycles of zonal wind are coherent with mountain-valley and sea-land breezes at low-levels and the easterly flow is predominant at mid-levels. Potential temperature anomalies appear to be related to gravity waves that modulate the diurnal cycle of precipitation in the region.

1 Introduction

The Chocó Low-Level Jet (ChocoJet) is a westerly low-level jet, an extension of the southwesterly cross-equatorial flow that converges over the far eastern Pacific and western Colombia, which exerts a strong modulation over the region's hydroclimate (Poveda and Mesa, 1997; 1999; 2000; Mapes *et al*., 2003a; 2003b; Vernenkar *et al*., 2003; Martínez *et al*., 2003; Martínez *et al*., 2006; Poveda *et al*., 2006; Pahnke *et al*., 2007; Bookhagen and Strecker, 2008;

Prange *et al*., 2010; Mollier-Vogel *et al*., 2013; Gimeno *et al*., 2016; Grados *et al*., 2018; Zhao and Keigwin, 2018; 2018; Gallego *et al*., 2018). The orographic interaction of ChocoJet with the downstream Andes has been linked to the existence of arguably the rainiest place on Earth, experiencing mean annual rainfall rates on the order of 13,000 mm, as documented by numerous studies (Murphy, 1939; Schmidt, 1952; Trojer, 1958; Arnett and Steadman, 1970; Snow, 1976, p. 371; Meisner and Arkin, 1987; Eslava, 1993, 1994; Janowiak *et al*., 1994; Poveda and Mesa, 2000; Mapes *et al*., 2003a, 2003b, Warner *et al*., 2003; Zuluaga and Poveda, 2004; González *et al*., 2006; Pahnke *et al*., 2007; Sakamoto *et al*., 2011; Álvarez-Villa *et al*., 2011; Durán-Quesada *et al*., 2012; Sierra *et al*., 2015; Jaramillo *et al*., 2017; King *et al*., 2017). ChocoJet feeds the highly biodiverse tropical rainforest that spreads over the Chocó-Darién region along the Colombian Pacific. Consistently, the region is home to communities exposed to extreme precipitation and recurrent flood events (Velasquez and Poveda, 2018; Jaramillo *et al*., 2017) and is one of the most critical hotspots around the world in terms of biodiversity loss (Myers *et al*., 2000). Scientific understanding of the role of ChocoJet in the region's hydroclimate and ecosystems has relied on remote sensing and reanalysis tools. Therefore, in situ observations to characterize the atmospheric circulation over these regions and help constrain reanalysis and operational models are of critical importance to accurately improve such understanding.

Sidebar 1 here.

During the boreal autumn, ChocoJet is related to the wet season over the western and central regions of Colombia (Poveda and Mesa, 2000; Rueda and Poveda, 2006). During this period, reanalysis shows a 4–6 m/s jet with its core at 925 hPa level. ChocoJet's diurnal, synoptic, and seasonal variability is influenced by regional circulation features, including the Caribbean Low-Level Jet (CLLJ; Poveda and Mesa, 1999; Amador, 2008; Poveda *et al*. 2014; Arias *et al*., 2015),

70 the Intertropical Convergence Zone (ITCZ) (Schneider *et al*., 2014) and the predominant easterly
71 flow over the Andes (López and Howell, 1967; Poveda *et al*., 2014). The ChocoJet has been linked
72 to frequent formation of nighttime and early morning Mesoscale Convective Systems (MCSs;
73 Mejía and Poveda, 2005; Zuluaga and Houze, 2015; Jaramillo *et al*., 2017) over western Colombia
74 and the Panama Bight, contributing approximately 57% of total rainfall in the region (Jaramillo *et*
75 *al*., 2017). At seasonal scales, the CLLJ interacts with ChocoJet and modulates the meridional
76 location of the ITCZ (Arias *et al*., 2015). At interannual scales, El Niño years tend to be associated
77 with weaker ChocoJet, thus contributing to the explanation of prolonged drier periods over the
78 Colombian Andes, with the reverse occurring during La Niña (Poveda and Mesa, 1997; 1999; 2000;
79 Poveda et al., 2001; Poveda *et al*., 2006), a finding that appears to be linked to a wetter precipitation
80 pattern observed during El Niño over northern Peru and Ecuador (Douglas *et al*., 2009). The
81 interannual variability of CLLJ is seasonally modulated. During boreal winter, the jet weakens
82 during El Niño and strengthens during La Niña. During boreal summer, the opposite relationships
83 have been found (Amador, 2006; Wang, 2007).

84 Despite the intricate atmospheric circulation patterns over the eastern equatorial Pacific and the
85 seemingly significant influence on the meteorology, hydrology, and ecosystems of northwestern
86 South America, no permanent or even experimental in situ upper-air measurements are available
87 to characterize the atmospheric profile and the ChocoJet flow vertical structure and variability. Fig.
88 1 shows the location of regional upper-air sounding systems, also indicating how spatially sparse
89 and infrequent operational real-time observations were during the last five years. Despite the
90 existence of Panamá and Guayaquil observations on the Pacific basin, different aspects (e.g.,
91 budget constraints, land mass distribution, logistical difficulties) have prevented the development
92 of a potentially better and denser upper-air soundings network. Thus, the ChocoJet Experiment

(CHOCO-JEX) was designed to start addressing the gap in observations through a set of field campaigns focused on upper–air soundings launched offshore from a research vessel and inland from the Universidad Tecnológica del Chocó at Quibdó (Fig. 1). Quibdó is the capital city of the Chocó province in Colombia and is located between the coastline and the westernmost Andes. CHOCO-JEX observations are crucial for a suite of diverse purposes including characterizing the atmospheric profile, evaluating reanalysis products, and assessing numerical simulation of the ChocoJet structure. Also, these observations will contribute to elucidating the role of gravity waves (Mapes *et al*., 2003b) in the diurnal cycle of precipitation over the region. Overall, CHOCO-JEX observations will contribute to improving the region's hydroclimate predictive capabilities.

CHOCO-JEX, mainly funded by COLCIENCIAS (Colombia Administrative Department of Science, Technology and Innovation), was made possible through a collaborative effort between Universidad Nacional de Colombia at Medellín, the General Maritime Directorate (DIMAR) of the Ministry of National Defense of Colombia, the Colombian Air Force (FAC), and the Desert Research Institute (DRI; Nevada, USA). Here we present a synthesis of the field campaigns conducted in 2016 and highlight the potential scientific understanding and the hypotheses driving the overall research project. Additionally, we identify some of the practical limitations and leverage opportunities related to the field campaigns. We present some preliminary results, discuss the capacity for future atmospheric field campaigns, and describe some of the education and outreach opportunities enabled through this project.

From socio-political conflicts to scientific wondering

For 52 years, Colombia endured an internal armed conflict between the national

government and leftist guerrillas, with added involvement of extreme right-wing paramilitary groups. This conflict left eight million victims, including 6.7 million displaced persons, more than 220,000 casualties, 74,000 victims of direct attacks on urban and rural populations, 11,000 victims of anti-personal mines, 45,000 forced disappearances, 10,000 torture victims, 30,000 kidnappings, and more than 2,000 massacres. Between 2012 and 2016 the Colombian government led by President Juan Manuel Santos and FARC (the largest and oldest armed rebel group) held talks in Havana, Cuba, and despite many difficulties, a peace agreement supporting a Definitive and Bilateral Cease of Fire and Hostilities was signed on November 24, 2016. The cost of the protracted warfare was enormous for Colombia, in the toll of victims and human suffering as well as in the diversion and depletion of national economic resources. Besides the internal conflict, inadequate funding for scientific research in Colombia has been caused by the historical disregard of governments about the importance of science, technology, innovation, and the humanities to improve the socio-economical conditions and enhance the cultural life of the country (Poveda, 2001), but also by ignoring the scientific community in the design of relevant scientific agendas (Poveda, 2004). In contrast, CHOCO-JEX brings together several educational, research, and public/defense institutions around relevant scientific challenges with huge potential benefits for all the institutions involved and the country in general. This collaborative effort constitutes an example of the benefits of cooperative research between the largest public university of Colombia and the military (Colombian Air Force and DIMAR) for the post-accord peace era. See Sidebar 2.

Sidebar 2 here

2 CHOCO-JEX

CHOCO-JEX is a multi-institutional collaborative effort, aimed at observing key aspects of the

low- to upper-level flow, thermodynamic structure, and temporal variability over the far eastern Pacific region, including the ChocoJet and inland over northwest Colombia. The experiment was conducted in 2016 and consisted of four intensive observational periods (IOPs), each lasting a week, two over the Pacific Ocean and two inland. Because of our interest in understanding diurnal and day-to-day variability, each IOP consisted of six hourly upper-air rawinsondes –measuring temperature, horizontal wind components, pressure, and relative humidity– distributed as shown in Table 1 (see Fig. 1). A website at https://sites.google.com/unal.edu.co/chocojex/home, currently under construction, will provide diverse data products and resources derived from CHOCO-JEX.

2.1 Experimental design: From the ideal to the real

CHOCO-JEX was designed to take advantage of the regular oceanographic survey carried out as part of the *Estudio Regional del Fenómeno El Niño* project (ERFEN), a regional coordinated effort between Chile, Peru, Ecuador, and Colombia aimed at monitoring physical and biological upper-ocean variables near the continental shelf (CPPS, 2017). The Colombian ERFEN component is coordinated and implemented by DIMAR. Typically, each country commits research vessels with at least one campaign during September–October. Seasonally, the ChocoJet is most intense during September-November (Poveda and Mesa, 1999; Poveda *et al*., 2014). Hence, our original plan was to carry out simultaneous maritime and land observations that coincided with the 2015 and 2016 ERFEN campaigns. Our interest to conduct simultaneous measurements during the 2015 Colombian ERFEN campaign, however, had to be adjusted because of unscheduled research vessel maintenance, shifting departure from early October 2015 to mid-January 2016.

Another striking challenge in this experiment was the unpredictable exchange rates, as the funding was provided in Colombian Pesos (COP) and the rawinsondes, receiver systems, and balloons were

quoted and purchased in U.S. dollars. There was an unexpected devaluation of the COP (nearly 40% from the time the proposal was submitted in 2014 to purchasing and acquisition in 2015) relative to the U.S. dollar, forcing to scale down the original field campaigns. Hence, from the original 168 rawinsondes and balloons (10-day per IOP), only 120 were purchased (7-day per IOP). Despite the outlined difficulties, 4 IOP's were developed successfully. Fig. 2 shows some activities carried out during CHOCO-JEX.

2.2 Instrumentation

The instrumentation acquired for the field campaigns comprised: MW41 Vaisala DigiCORA Sounding System, Ground Check Device RI41, Vaisala Radiosondes RS41-SG and Meteorological Balloons TA200. The sounding system allowed us to measure vertical profiles of atmospheric pressure, temperature, relative humidity, magnitude and wind direction.

The ARC Gorgona vessel from DIMAR was the launching platform during the oceanic campaigns. For more than 50 years, the ARC Gorgona has accomplished different operational and research tasks regarding hydrography, maritime signposting and support to the Colombian National Navy. During the ERFEN campaigns, ARC Gorgona aims to measure diverse vertical and horizontal column water characteristics.

3 Field Campaign Achievements and Preliminary Results

The original CHOCO-JEX plan was to gather observations during the enhanced ChocoJet season (September-November) to increase the chance of observing environmental conditions that resembled enhanced low-level southwesterly flow. All IOPs were deployed throughout rapidly

changing ENSO conditions, as classified by the Oceanic Niño Index (ONI; CPC/NOAA). However, each of the four campaigns was heavily constrained by diverse unscheduled logistical hurdles (some of which are highlighted above). The synoptic intraseasonal, seasonal, and interannual identifiable environmental conditions during each campaign included the following:

1. IOP1 (January 15-22, 2016): This IOP was carried out during one of the strongest El Niño events ever recorded (L'Heureux *et al.*, 2017). According to the Institute of Hydrology, Meteorology and Environmental Studies of Colombia (IDEAM, January 2016), January, 2016, was characterized by anomalously dry conditions over most of Colombia. Climatologic studies have shown that during El Niño conditions, most of Colombia is typically associated with relatively dry conditions (Poveda *et al.*, 2001; 2011; Bedoya-Soto *et al*., 2018), while the coasts of northern Peru and southwest Ecuador experience wetter conditions (Sulca *et al*., 2017). Fig. 3a shows wind anomalies during January, 2016, highlighting several regional patterns, including: stronger than normal Panama Jet (Xie *et al*., 2005), the *Corriente de los Andes Orientales* (*CAO* or Eastern Andes Jet, also known as *Llanos Jet*; Montoya, 2001; Torrealba and Amador, 2010), which constitutes the northernmost leg of the South American Low Level Jet (SALLJ) (Vera et al., 2006); and weaker than normal CLLJ (Amador, 2006; Wang, 2007), Papagayo and Tehuantepec Jet (Xie *et al*., 2005). These anomalous flow conditions over the eastern Pacific resembled those of the 1997/98 El Niño event (Douglas *et al.*, 2009). In particular, IOP1 showed a relatively weak ChocoJet and dominated by a stronger Panama Jet.
2. IOP2 (June 25 – July 1, 2016): IDEAM reported that precipitation over Colombia was below normal for this time of the year, with near neutral ENSO conditions over the Tropical Pacific (IDEAM, June 2016). Additionally, IDEAM indicated that the ITCZ was displaced

to the north over the Central America and northern Colombian Pacific coast enabling low-level southwesterlies to reach the far eastern Pacific region (Poveda and Mesa, 1999). During this IOP, the CLLJ was anomalously strong.

3. IOP3 (October 15-21, 2016): A weak La Niña conditions were predominant during October, 2016. IDEAM reported normal precipitation over western Colombia, the ITCZ trough axis was located over the EPAC (6°N–15°N), scattered precipitation events over the northern and central Colombian Pacific coast (IDEAM, October, 2016). At a regional scale, not tropical storm activity occurred near or during this IOP.
4. IOP4 (November 21-28, 2016): IDEAM reported that the Pacific Colombian coast showed near-normal precipitation conditions, likely influenced by the La Niña phase over the Tropical Pacific (IDEAM, November, 2016). Regional circulation features during this month (Figure 3b) resembled those shown by Arias *et al*. (2015) for the 2010–2012 La Niña event dominated by a relatively stronger than normal ChocoJet and weaker than normal CLLJ. Preliminary analysis suggests that both of these regional features were also observed during IOP4 (Fig. 3). Tropical Storm Otto was located over western Caribbean Sea and transition into a hurricane system before moving away over Central America and the Pacific basin (November 20–26). Thus, we hypothesized that the first half of IOP4 was influenced by Otto's circulation.

Figs. 4 and 5 (panels a and c) show the zonal moisture flux during the four IOPs. A shallow westerly component around 50 g/kg*m/s at low levels was observed during IOP1, showing a diurnal signal on January 18–19 associated with the proximity to land (see Fig. 1). An easterly component (50 g/kg*m/s) was prevalent at mid-levels and in some cases at low-levels. At sub-daily timescales, IOP2 and IOP3 showed relatively large diurnal variability, likely related to land-sea and valley-

mountain breezes – with a stronger afternoon westerly component around 50–100 g/kg*m/s and a weaker early morning easterly component around 20 g/kg*m/s. This diurnal cycle was stronger during IOP3 than during IOP2. At mid-levels, the observed easterly moisture flux was up to 100 g/kg*m/s during IOP2, whereas IOP3 showed values around 20 g/kg*m/s. In contrast, westerly moisture flux (50 g/kg*m/s) at low levels and easterly moisture flux (15 g/kg*m/s) at mid-levels prevailed along with high variability in wind profile during IOP4.

Since the IOP4 shows a strong ChocoJet (Figs 4 and 5) we examined composites of circulation along with Vertical Integrated Water Vapor from MERRA reanalysis at 850 hPa and IR satellite images (Fig. 6). This IOP shows two different pronounced synoptic conditions: (i) predominant meridional and drier flow likely influenced by Otto's depression between November 21 and 24; and (ii) westerly and wetter flow during November 25 to 28. A particular feature during the IOP4 is that convection activity and precipitation over western Colombia was suppressed until November 24th. Later during (ii), a wet spell of scattered convection and sustained MCSs developed on November 25 and 27 over northern Colombian Pacific. Overall, MERRA shows a deeper low-level southwesterly flow than seen in observations during (i). At any rate, both datasets coincide with strong southwesterlies during (ii) .

Observations show during (i) a relatively weaker westerly (no significant differences in meridional flow were observed) and low-level moisture flux of 50 g/kg*m/s, in combination with an easterly moisture flow at mid-levels; and (ii) a deeper and more intense westerly moisture flux of 80 to 100 g/kg*m/s. We hypothesize that after Otto moved away from the region, a more zonal low-level flow was established, with enhanced southwesterly moisture flow favoring moisture flux convergence and orographic forcing. Coinciding with this period of enhanced precipitation, however, were observed larger convection indices – such as Convective Available Potential Energy

254 (CAPE) and helicity (not shown).

255 Figs. 4 and 5 (panels b and d) also show the vertical distribution of the zonal wind component and
256 specific humidity averaged during each IOP, along with the same vertical profiles using ERA-I and
257 MERRA products. IOP1 and IOP2 showed weak westerly flow at low levels (<2 m/s) which was
258 deeper (up to 900 hPa) during IOP2. At mid-levels, easterlies were predominant between 800 hPa
259 and 300 hPa with maximum values around 10 m/s at 500 hPa. In general, IOP3 and IOP4 showed
260 low-level southwesterlies that resembled ChocoJet conditions (Poveda and Mesa 1999). Both IOP3
261 and IOP4 showed a weak, low-level, zonal wind (2–4 m/s) extending from the surface up to 850
262 hPa with maximum around 925–950 hPa. Mid-level easterly flow was observed above 850 hPa
263 during both campaigns, with values below 5 m/s. Specific humidity profiles were similar during
264 all IOP's with exception of IOP4, which showed a drier profile from low-to-mid levels and values
265 below 10 g/kg at low-levels in connection to Otto (Fig. 6). Observations showed high day-to-day
266 variability with stronger westerlies at low-levels during October 17–18th and November 26–27
267 reaching values of 6–7 m/s (not shown). During IOP4, low-level westerlies and specific humidity
268 increased after Otto moved away from the region on November 26th.

269 Overall, ERA-Interim and MERRA show the vertical variability of the zonal wind and specific
270 humidity during each IOP, however, some bias can be distinguished such as the more pronounced
271 and deeper ChocoJet as represented by MERRA during inland campaigns. Oceanic campaigns
272 exhibited better agreement than those over land, likely associated with misrepresentation of
273 dynamic and thermodynamic processes over complex terrain. However, during IOP4, both
274 reanalyses exhibit a ChocoJet-like feature, with peak zonal wind between 4-5 m/s at 950-975 hPa;
275 MERRA resolves a deeper and about 2 m/s stronger Jet (Fig. 5).

276 A striking feature help distinguish the maritime from inland atmospheric environments. Over the

277 ocean, IOP1 and IOP4 showed a shallow westerly wind component, except for the relatively active
278 ChocoJet period in IOP4 during November 25-28 (Fig. 5). In contrast, IOP2 and IOP3 showed
279 deeper westerly flow, reaching up to 800 hPa, somehow affected by the orographic barrier located to the
280 east that prevents easterlies at low levels.

281 3.1. Observed Diurnal Variability

282

283 At diurnal scales, moister and cooler westerlies at low-levels (from ChocoJet) prevail during
284 afternoon hours, in combination with warmer and drier easterlies at mid-levels that cause highly
285 unstable conditions inducing convection inland (Fig. 7). In general, this afternoon circulation is
286 consistent with the diurnal cycle near the coast shown by inland observations (Fig. 8). At low-
287 levels, variability of the winds was consistent with valley-mountain and land-sea contrasts. During
288 IOP2, a shallow westerly late afternoon flow of 2-3 m/s contrasts the 1 m/s easterly nighttime flow,
289 likely related to the drainage current from the sierra to the east. Similar diurnal pattern is observed
290 during IOP3 but a more accentuated and deeper late afternoon westerly flow. At mid-levels, with
291 a noticeable easterly flow dominated all IOPs with more intense flow during IOP1 and IOP2 than
292 during IOP3 and IOP4. IOP1 showed a weak low-level westerly component in the afternoon (19:00
293 LST, 00:00 UTC) and low-level easterly flow during morning hours. IOP2 and IOP3 showed a
294 weak low-level westerly wind component, that was enhanced during the afternoon (19:00 LST;
295 especially during IOP3) apparently because of sea breeze in combination with valley-mountain
296 local circulation. It is interesting that low-level afternoon flow was larger during IOP3 (wet season)
297 than IOP2 (dry season), recalling that both inland campaigns were carried out at the western flank
298 of Western range of the Andes. In contrast, Lopez and Howell (1967) argued katabatic winds are
299 greater during the dry season over the eastern flank of the Western range (southern location of the

inland field campaigns). During IOP4, the westerly wind component was predominant throughout the day. Westerlies were stronger during the afternoon (19:00 LST), however, and weaker during morning hours (7:00 LST, 12:00 UTC). Mid-level winds in IOP3 showed relatively large diurnal variability with weak westerlies at midnight (01:00 LST, 6:00 UTC) and easterlies at early afternoon (13:00 LST, 18:00 UTC). Reanalysis products show easterlies all day long (not shown).

3.2. Observational Clues of the Gravity Waves

The diurnal variations of zonal wind shown in Fig. 8 has been related to a mechanism that appears to be linked to the diurnal cycle of precipitation in the region (Mapes et al. 2003b). Over the Colombian Western range of the Andes, late-afternoon showers developed, likely driven by sea-valley breeze (Jaramillo *et al*., 2017) combined with the rather weak but steadier ChocoJet. In contrast, late night and morning convection over coastal waters has been related to mid-level gravity waves developed by the daytime mixed layer over the western Andes mountain range (Yang and Slingo, 2001; Mapes *et al*., 2003b). The role of gravity waves triggering offshore convection has been studied in other regions with similar characteristics as western Colombia (Love *et al*., 2011; Li and Carbone, 2015; Zhou and Wang, 2006; Yokoi *et al*., 2017). For instance, Yokoi *et al*. (2017) used soundings to show that the lower troposphere offshore Sumatra Island tends to cool down during late afternoon before the onset of precipitation.

Fig. 9 shows the observed potential temperature profile after removing the mean diurnal cycle averaged during each IOP. Not surprisingly, inland campaigns (IOP2 and IOP3) showed relatively stronger warm daytime theta anomalies extending from the surface to 850 hPa. Absolute surface maxima developed at 19:00 LST for IOP2 and 13:00 LST for IOP3 as determined by 6-hourly observations. We hypothesize that this surface asymmetry was likely due to differences in

cloudiness and convection activity during the campaigns. Despite being developed over the ocean, the maritime campaigns showed a diurnal but weaker thermal disturbance, even at high levels, with IOP4 showing a weaker thermal disturbance than IOP1. Theta disturbances for IOP4 were composited using soundings located farther offshore than IOP1. Of note in Fig. 9 is the inland mid-level layer (850–750 hPa) discontinuity in daytime heating, related to flow direction change with height, suggesting the presence of two different air masses with a westerly (Fig. 8), wetter, and slower heating response bottom layer, contrasting an easterly, drier and warmer theta mid-level layer right above. A striking feature in Fig. 9 is the lagged heating differences between land and maritime soundings, suggesting the existence of a mid-level westward thermal propagation, arguably because of the postulated gravity waves.

Potential temperature anomalies between 850 and 900 hPa in IOP4 revealed cooling at early morning likely related to the initiation of convective activity offshore (IR images show cloud occurrence at 7:00 LST), as proposed by Mapes *et al*. (2003b). We hypothesize that the anomalous cooling is likely caused by vertical advection in the atmosphere favoring convection conditions, as is the case in Sumatra (Yokoi *et al*., 2017). They argue that both cooling and vertical ascent are caused by shallow gravity waves with a horizontal phase speed of 8–10 m/s, such hypothetical gravity waves are consistent with the timing of the late-afternoon cooling observed over ocean. The processes are triggered by evaporative cooling from inland convective systems that generate gravity waves with ascending wave fronts in the lower troposphere and that propagate offshore horizontally (Hassim *et al*., 2016). Note that for Colombia's case, the cooling is lagged with respect to Sumatra – showing the cooling at early morning hours (Fig. 9). Also, larger convective instability indices (CAPE, surface-6 km vertical shear and helicity) were observed during late afternoon (19:00 LST) in IOP1, IOP2, and IOP3 and early morning (7:00 LST) in IOP4, when convection started on

coastal waters and land, respectively (not shown). Unfortunately, our observations were not simultaneous and to investigate the role of the cooling at low levels in the formation of convection, model simulations are required. Future work will include the analysis of hourly simulations at different spatial scales during the IOPs that allow comparing simultaneous atmospheric profiles on ocean and land. Temperature, humidity, wind anomalies will help us to investigate the association of the gravity waves with the convection generation. Likewise, observations provided from CHOCO-JEX will evaluate the model performance.

4 Final Remarks and Summary

CHOCO-JEX provided upper-air observations over the far eastern tropical Pacific from four intensive observational periods, two carried out over a research vessel following operational reconnaissance maritime transects and two inland (Quibdó, Colombia). Upper-air soundings were performed four times per day with an average of seven days per IOP. Data analysis and assimilation including these observations, in combination with simulation experiments, are currently in progress and are intended to improve our understanding of the mechanisms responsible for the genesis and diurnal timing of the convection organization in one of the rainiest regions on Earth. Preliminary results and remarks are as follows:

1) CHOCO-JEX provided atmospheric soundings during different seasonal and synoptic conditions. IOP1 was performed during a particularly strong El Niño event (2015–2016).
2) Maritime observations during IOP4 provided the first observational evidence of the southwesterly low-level ChocoJet. The persistence and intensity of ChocoJet was modulated by hurricane Otto that developed over the western Caribbean.
3) Land-atmosphere interactions (IOP2 and IOP3) revealed a deeper westerly flow and

stronger diurnal cycle than observed over the ocean (IOP1 and IOP4).

4) Noticeable sea-land and valley-mountain local circulation was observed as a response to the surface thermal contrast during IOP1 and IOP3.

5) Flow and thermal diurnal variations at 850 hPa were observed with an intriguing delay (cooling at early morning hours) of maritime responses relative to inland mean diurnal anomalies, possibly supporting the role of the Andes convective and boundary layer processes in the far east Pacific convective environment. A question remains as to whether the observed cooling either occurs by advection, propagation of a gravity wave disturbance (Mapes *et al*., 2003b), or a combination of both processes. Further analysis may provide an answer to this question.

Further examination of these CHOCO-JEX observations, including the comparison against reanalysis, is necessary. Recall that IOPs were deployed during different seasons and that maritime soundings were averaged despite the constantly changing sounding location. Another research paper using data assimilation procedures and Lagrangian trajectories is being prepared to further explore the significance of the outlined features, since they may help elucidate the gravity wave genesis hypothesis (Mapes *et al*., 2003b) and its role on convective organization postulated by simulation studies in the region. CHOCO-JEX will help evaluate and constrain mesoscale and high-resolution simulations to improve understanding of the role of boundary layer and convective processes over the Andes, including the effect of latent heat released during organized convection systems in triggering westward-moving, mid-level thermal disturbances propagating from land to the ocean, as proposed by Mapes *et al*. (2003b). Other questions of interest include: What is the influence of heat fluxes and PBL on the observed rain patterns along the Colombian Pacific coast?

What are the role of the Choco-Darien rainforests in terms of water and energy budgets over the Colombian Pacific? What is the relation of moisture flow to generation of MCSs and orographic rainfall in the Colombian Pacific region? How important is the ChocoJet to explain rainfall patterns in Colombia?

While improving our knowledge of the relevant circulation features in the region, CHOCO-JEX also addresses the communication and interaction gap between local academia/researchers and end-user institutions. The tools and equipment acquired by CHOCO-JEX, the established local and international collaborations, and the resulting data sets are building research capacity and potentially can further support understanding of the region's hydrometeorology. Observations generated by these campaigns have been distributed to key operational and research centers in the region and will be distributed to any interested researchers and institutes.

Acknowledgements

It is a pleasure to acknowledge the scientists, students, collaborators, and local volunteers from the Universidad Nacional de Colombia, Universidad Tecnológica del Chocó, DIMAR, FAC, DRI who participated in the planning, execution, and data analysis for CHOCO-JEX. Special thanks are due to Brian E. Mapes for encouraging us to explore relevant ideas and to Leswis Cabeza, Carlos Forero, and Mauricio Jiménez for their collaboration during the field campaigns. CHOCO-JEX was partially funded by the Colombian Administrative Department of Science, Technology and Innovation (COLCIENCIAS) and its Science, Technology, and Innovations in Geosciences program (N°660 of 2014). DIMAR, FAC, DRI and Universidad Nacional de Colombia contributed with invaluable in-kind support during the whole CHOCO-JEX experiment. We thank the three anonymous reviewers and the editor, Ed Zipser, for providing comments that significantly

improved this paper.

References

Alvarez-Villa, O. D., J. I. Vélez, and G. Poveda, 2011: Improved long-term mean annual rainfall fields for Colombia, *International Journal of Climatology*, **31**, 2194–2212.

Amador, J., E. J. Alfaro, O. G. Lizano and V. O. Magaña, 2006: Atmospheric forcing of the eastern tropical Pacific: A review. *Progress in Oceanography*, **69**(2-4), 101–142.

Amador, J., 2008: The Intra-Americas Sea low-level jet: overview and future research. *Annals of the New York Academy of Sciences*, **1146**, 153–188. http://doi.org/10.1196/annals.1446.012

Arias, P. A., J. A. Martínez and S. C. Vieira, 2015: Moisture sources to the 2010–2012 anomalous wet season in northern South America. *Climate Dynamics*, **45**, *2861–2884*. http://doi.org/10.1007/s00382-015-2511-7

Arnett, A.B. and C.R. Steadman, 1970: Low-level wind flow over eastern Panama and northwestern Colombia, *ESSA Technical Memorandum ERLTM-ARL 26*, U. S. Department of Comerce, Environmental Science Services Administration Research Laboratories, Air Resources Lab., Silver Spring, Maryland, 73 pp.

Bedoya-Soto, J. M, G. Poveda, K. Trenberth and J. Vélez, 2018: Interannual hydro-climatic variability and the 2009–2011 extreme ENSO phases in Colombia: From Andean glaciers to Caribbean low-lands. *Theoretical and Applied Climatology*. https://doi.org/10.1007/s00704-018-2452-2.

Bookhagen, B. and M.R. Strecker, 2008: Orographic barriers, high-resolution TRMM rainfall, and relief variations along the eastern Andes. *Geophysical Research Letters*, **35**(6), L06403.

Coelho A. S., C. Uvo, and T. Ambrizzi, 2002: Exploring the impacts of the Tropical Pacific SST

on the precipitation patterns over South America during ENSO periods. *Theoretical and Applied Climatology*, **71**, 185-197. https://doi.org/10.1007/s007040200004

CPPS, 2017. *Boletín de Alerta Climático* 321, 20 p., https://www.dhn.mil.pe/Archivos/Oceanografia/BAC/06-2017.pdf (Available in Spanish)

Douglas, M. W., J. Mejía, N. Ordinola, and J. Boustead, 2009: Synoptic variability of rainfall and cloudiness along the coasts of northern Peru and Ecuador during the 1997/98 El Niño event. *Monthly Weather Review*, **137**(1), 116–136. http://doi.org/10.1175/2008MWR2191.1

Durán-Quesada, A. M., M. Reboita, and L. Gimeno, 2012: Precipitation in tropical America and the associated sources of moisture: a short review. *Hydrological Sciences Journal*, **57**(4), 612–624. http://doi.org/10.1080/02626667.2012.673723

Eslava, J. 1993: Some particular climatic features of the Colombian Pacific region. *Atmósfera*, **17**, 45-63.

Eslava, J., 1994; Climatología del Pacífico Colombiano, *Academia Colombiana de Ciencias Geofísicas, Colección Eratóstenes*, **No.1**, 79 p.

Gallego, D., R. García-Herrera, F. D. P. Gómez-Delgado, P. Ordoñez-Perez, P. and Ribera, 2018: Tracking the Choco jet since the 19th Century by using historical wind direction measurements, *Earth System Dynamics*. https://doi.org/10.5194/esd-2018-54 (in review).

Gimeno, L., F. and Coauthors, 2016: Major mechanisms of atmospheric moisture transport and their role in extreme precipitation events. *Annual Review of Environment and Resources*, **41(**1), 117-141.

González, C., L.E. Urrego and J.I. Martínez, 2006: Late Quaternary vegetation and climate change

in the Panama Basin: Palynological evidence from marine cores ODP 677B and TR 163-38, *Palaeogeography, Palaeoclimatology, Palaeoecology*, **234**(1), 62-80.

Grados, C., A. Chaigneau, V. Echevin, and N. Dominguez, 2018: Upper ocean hydrology of the Northern Humboldt Current System at seasonal, interannual and interdecadal scales. *Progress in Oceanography*, 165, 123-144.

Hassim, M. E. E., T. P. Lane, and W. W. Grabowski, 2016: The diurnal cycle of rainfall over New Guinea in convection permitting WRF simulations. *Atmospheric Chemistry and Physics*, **16**, 161– 175, https://doi.org/10.5194/acp-16-161-2016.

Hastenrath, S. 1991. *Climate Dynamics of the Tropics*, 488 p. Kluwer, Dordretcht.

IDEAM, January 2016: *Climate Bulletin* (Available in Spanish).

IDEAM, June 2016: *Climate Bulletin* (Available in Spanish).

IDEAM, October 2016: *Climatic Bulletin* (Available in Spanish).

IDEAM, November 2016: *Climatic Bulletin* (Available in Spanish).

Janowiak, J. E., P.A. Arkin, and M. Morrissey, 1994: An examination of the diurnal cycle in oceanic tropical rainfall using satellite and in situ data, *Monthly Weather Review*, **122**, 2.296-2.311.

Jaramillo, L., G. Poveda, and J. F. Mejía, 2017: Mesoscale convective systems and other precipitation features over the tropical Americas and surrounding seas as seen by TRMM. *International Journal of Climatology*, **37**(S1), 380–397. https://doi.org/10.1002/joc.5009

King, M. J., M.C. Wheeler, and T. P. Lane, 2017: Mechanisms linking global 5-day waves to tropical convection. *Journal of the Atmospheric Sciences*, **74**, 3679–3702,

https://doi.org/10.1175/JAS-D-17-0101.1

L'Heureux, M.L., K. Takahashi, A.B. Watkins, A.G. Barnston, E.J. Becker, T.E. Di Liberto, F. Gamble, J. Gottschalck, M.S. Halpert, B. Huang, K. Mosquera-Vásquez, and A.T. Wittenberg, 2017: Observing and Predicting the 2015/16 El Niño. *Bull. Amer. Meteor. Soc.*, **98**, 1363–1382, https://doi.org/10.1175/BAMS-D-16-0009.1

Li, Y., and R. E. Carbone, 2015: Offshore propagation of coastal precipitation. *Journal of the Atmospheric Sciences*, **72**(12), 4553–4568. https://doi.org/10.1175/JAS-D-15-0104.1

López, M. E. and W. E. Howell, 1967: Katabatic winds in the Equatorial Andes. *Journal of the Atmospheric Sciences*, **24**(1), 29–35. http://doi.org/10.1175/1520-0469(1967)024<0029:KWITEA>2.0.CO;2

Love, B. S., A. J. Matthews, and G. M. S. Lister, 2011: The diurnal cycle of precipitation over the Maritime Continent in a high-resolution atmospheric model. *Quarterly Journal of the Royal Meteorological Society*, **137**(657), 934–947. https://doi.org/10.1002/qj.809

Mapes, B. E., T. T. Warner, and M. Xu, 2003a: Diurnal patterns of rainfall in northwestern South America. Part I: Observations and Context. *Monthly Weather Review*, **131**(5), 799–812.

Mapes, B. E., T. T. Warner, and M. Xu, 2003b: Diurnal patterns of rainfall in northwestern South America. Part III: Diurnal gravity waves and nocturnal convection offshore. *Monthly Weather Review*, **131**(5), 830–844.

Martínez, I., L. Keigwin, T. T. Barrows, Y. Yokoyama, and J. Southon, 2003: La Niña like conditions in the eastern equatorial Pacific and a stronger Choco jet in the northern Andes during the last glaciation, *Paleoceanography and Paleoclimatology*, **18**(2), 1033 doi:10.1029/2002PA000877.

503 Martínez, J. I., et al. (2006), Foraminifera and coccolithophorid assemblage changes in the Panama
504 Basin during the last deglaciation: Response to sea-surface productivity induced by a transient
505 climate change, *Paleogeography, Paleoclimatology, Paleoecology*, **234**(1), 114– 126.

506 Meisner, B.N., and P.A. Arkin, 1987: Spatial and annual variations in the diurnal cycle of large-
507 scale tropical convective clouds and precipitation, *Monthly Weather Review*, **115**, 2.009-2.032.

508 Mejía, J. F. and G. Poveda, 2005: Atmospheric environments of mesoscale convective systems
509 over Colombia during 1998 according to the TRMM mission and the NCEP / NCAR re-
510 analysis. *Journal of the Colombian Academy of Exact, Physical and Natural Sciences*,
511 **29**(113), 495–514. (Available in Spanish).

512 Mollier-Vogel, E., G. Leduc, T. Böschen, P. Martinez, R. Schneider, 2013: Rainfall response to
513 orbital and millennial forcing in northern Peru over the last 18 ka, *Quaternary Science*
514 *Reviews*, **76**, 29-38.

515 Montoya, G. J., J. Pelkowski, and J. A. Eslava, 2001: Sobre los alisios del noreste y la existencia
516 de una corriente en el piedemonte oriental Andino. *Revista de la Academia Colombiana de*
517 *Ciencias Exactas, Físicas y Naturales*, **25**(96): 363-370.

518 Murphy, R. C, 1939: The Littoral of Pacific Colombia and Ecuador. *Geographical Review, JSTOR*,
519 **29**(1), 1–33.

520 Myers, N., R. A. Mittermeier, C. G. Mittermeier, G. A. da Fonseca, and J. Kent, 2000: Biodiversity
521 hotspots for conservation priorities. *Nature*, **403**(6772), 853–8.
522 http://doi.org/10.1038/35002501

523 Pahnke, K., J. P. Sachs, L. Keigwin, A. Timmermann, and S.-P. Xie (2007), Eastern tropical Pacific
524 hydrologic changes during the past 27,000 years from D/H ratios in alkenones,

Paleoceanography and Paleoclimatology, **22**(4), PA4214, doi:10.1029/2007PA001468.

Poveda, G. 2001: Leaders need to realize that science can offer a route out of poverty. *Nature*, **409**(6821), 662–662. https://doi.org/10.1038/35055714

Poveda, G., 2004: Science priorities ignore Colombia's water needs. *Nature*, **431**(7005), 125–125. https://doi.org/10.1038/431125a

Poveda, G., L. Jaramillo, and L. F. Vallejo, 2014: Seasonal precipitation patterns along pathways of South American low-level jets and aerial rivers. *Water Resources Research*, **50**, 98–118. http://doi.org/ 10.1002/2013WR014087

Poveda, G., and O. J. Mesa, 1996: The extreme phases of the ENSO phenomenon (El Niño and La Niña) and their influence on Colombian hydrology (In Spanish). *Hydraulic Engineering in Mexico*, **XI**(1), 21–37.

Poveda, G., and O. J. Mesa, 1997: Feedbacks between hydrological processes in tropical South America and large-scale ocean-atmospheric phenomena, *Journal of Climate*, **10**(10), 2690 – 2702.

Poveda, G., and O. J. Mesa, 1999: The westerly low-level Choco Jet and two toher atmospheric jets over Colombia: Climatology and variability during ENSO phases (In Spanish). *Revista de la Academia Colombiana de Ciencias Exactas, Físicas y Naturales*, **23**(89) 517-528.

Poveda, G., and O. J. Mesa, 2000: On the existence of Lloró (the rainiest locality on Earth): Enhanced ocean-land-atmosphere interaction by a low-level jet. *Geophysical Research Letters.*, **27**(11), 1675–1678. http://doi.org/10.1029/1999GL006091

546 Poveda, G., D. M. Álvarez, and O. A. Rueda, 2011: Hydro-climatic variability over the Andes of
547 Colombia associated with ENSO: A review of climatic processes and their impact on one of
548 the Earth's most important biodiversity hotspots. *Climate Dynamics*, **36**(11-12), 2233-2249.
549 https://doi.org/10.1007/s00382-010-0931-y

550 Poveda, G., P. R. Waylen, and R. Pulwarty, 2006: Modern climate variability in northern South
551 America and southern Mesoamerica. *Paleogeography, Paleoclimatology, Paleoecology*, **234**,
552 3–27.

553 Poveda, G., A. Jaramillo, M. M. Gil, N. Quiceno, and R. I. Mantilla, 2001: Seasonality in ENSO-
554 related precipitation, river discharges, soil moisture, and vegetation index in Colombia. *Water*
555 *Resources Research*, **37**(8), 2169–2178. https://doi.org/10.1029/2000WR900395

556 Poveda, G., N. E. Graham, P. R. Epstein, W. Rojas, M. L. Quiñones, I. D. Vélez, and W. J. M.
557 Martens, 2000: Climate and ENSO variability associated with vector-borne diseases in
558 Colombia. *El Niño and the Southern Oscillation, Multiscale Variability and Global and*
559 *Regional Impacts*. Cambridge University Press, 183-204.

560 Prange, M., S. Steph, M. Schulz, L.D. Keigwin, 2010: Inferring moisture transport across Central
561 America: Can modern analogs of climate variability help reconcile paleosalinity records?
562 *Quaternary Science Reviews*, **29**(11)**,** 1317-1321

563 Romero-Centeno, R, J. Zavala-Hidalgo, and G. B. Raga, 2007: Midsummer gap winds and low-
564 level circulation over the eastern tropical Pacific. *J. Climate*, **20**, 3768-3784.

565 Rueda, O. A. and G. Poveda, 2006: Spatial and temporal variability of the Choco Low Level Jet
566 and its effect on the hydroclimatology of the Colombian Pacific region. *Colombian*
567 *Meteorology*, **10**, 132–145. (Available in Spanish).

568 Sakamoto, M. S., T. Ambrizzi, and G. Poveda, 2011: Moisture sources and life cycle of convective
569 systems over western Colombia. *Advances in Meteorology*, **2011**, 1–11.
570 http://doi.org/10.1155/2011/890759

571 Schmidt, R.D., 1952: Die Niederschlagsverteilung im Andinen Kolumbien. *Bonner Geogr.*
572 *Abhandl*., **9**, 99-119.

573 Schneider, T., T. Bischoff, and G. H. Haug, 2014: Migrations and dynamics of the intertropical
574 convergence zone. *Nature*, **513**(7516), 45–53. http://doi.org/10.1038/nature13636

575 Sierra, J. P., P. A. Arias, and S. C. Vieira, 2015: Precipitation over Northern South America and
576 Its Seasonal Variability as Simulated by the CMIP5 Models, *Advances in Meteorology*, **2015**,
577 1-22. https://doi.org/10.1155/2015/634720.

578 Snow, J. W. 1976: The climate of northern South America. *Climates of Central and South America*,
579 W. Schwerdtfeg, Ed. Elsevier, pp. 295 – 403.

580 Sulca, J., K. Takahashi, J. C. Espinoza, M. Vuille, and W. Lavado-Casimiro, 2018: Impacts of
581 different ENSO flavors and tropical Pacific convection variability (ITCZ, SPCZ) on austral
582 summer rainfall in South America, with a focus on Peru. *International Journal of Climatology*,
583 **38**(1), 420–435. https://doi.org/10.1002/joc.5185

584 Torrealba E. R. and J. A. Amador, 2010: La corriente en chorro de bajo nivel sobre los Llanos
585 Venezolanos de Sur América. *Revista de Climatología*, **10**,1-10.

586 Trojer, H., 1958: Meteorología y Climatología de la vertiente del Pacífico Colombiano. *Revista de*
587 *la Academia Colombiana de Ciencias Exactas, Físicas y Naturales*, **10**(40), 199-219.

588 Velásquez, M. and G. Poveda, 2018: Estimación del balance hídrico de la región Pacífica

589 Colombiana. *Revista Dyna*. (Submitted in Spanish).

590 Vera, C., et al., 2006: The South American Low-Level Jet Experiment, *Bulletin of the American*
591 *Meteorological Society*, **87**, 63 –77, doi:10.1175/BAMS87-1-63

592 Vernekar, A. D., B. Kirtman and M. Fennesy, 2003: Low-level jets and their effects on the South
593 American summer climate as simulated by the NCEP Eta model, *Journal of Climate*, **16**(2),
594 297– 311.

595 Wang, C. (2007). Variability of the Caribbean low-level jet and its relations to climate. *Climate*
596 *Dynamics*. **29**, 411-422. doi: 10.1007/s00382-007-0243-z

597 Warner, T. T., B. E. Mapes, and M. Xu, 2003: Diurnal patterns of rainfall in northwestern South
598 America. Part II: Model simulations. *Monthly Weather Review*, **131**, 813–829.

599 Yang, G. Y., and J. Slingo, 2001: The diurnal cycle in the Tropics. *Monthly Weather Review.*, **129**,
600 784–801. https://doi.org/10.1175/1520-0493(2001)129<0784:TDCITT>2.0.CO;2

601 Yokoi, S., S. Mori, M. Katsumata, B. Geng, K. Yasunaga, F. Syamsudin and K. Yoneyama, 2017:
602 Diurnal cycle of precipitation observed in the western coastal area of Sumatra island: Offshore
603 preconditioning by gravity waves. *Monthly Weather Review*, **145**(9), 3745–3761.
604 https://doi.org/10.1175/MWR-D-16-0468.1

605 Zhao, N., and L. D. Keigwin, 2018: An atmospheric chronology for the glacial-deglacial Eastern
606 Equatorial Pacific. *Nature Communications*, **9**, 3077.

607 Zhou, L., and Y. Wang, 2006: Tropical Rainfall Measuring Mission observation and regional
608 model study of precipitation diurnal cycle in the New Guinean region. *Journal of Geophysical*
609 *Research*, **111**(D17), D17104. https://doi.org/10.1029/2006JD007243

610 Zuluaga, M. D., and G. Poveda, 2004: Diagnóstico de sistemas convectivos de mesoescala sobre
611 Colombia y el océano Pacífico oriental durante 1998-2002 (Diagnostics of meso-scale
612 convective systems over Colombia and the eastern Pacific Ocean during 1998-2002). *Avances*
613 *en Recursos Hidráulicos*,**11**, 145–160.

614 Zuluaga, M. D., and R. A. Houze, 2015: Extreme convection of the near-equatorial Americas,
615 Africa, and adjoining oceans as seen by TRMM. *Monthly Weather Review*, **143**(1), 298–316.
616 http://doi.org/10.1175/MWR-D-14-00109.1

617

618 Sidebar 1: Choco and Caribbean Low-Level Jets Climatology

619

620 The existence of the Choco Low-Level Jet is related to the southwesterly branch of the southerly
621 cross equatorial flow over the far Eastern Pacific (ChocoJet; Poveda and Mesa, 1999, 2000). It is
622 driven by the seasonal variability in the gradient of Sea Surface Temperatures (SST) between the
623 Niño 1+2 region and the Colombian Pacific, which is stronger during September-November and
624 weaker during February-March (Poveda and Mesa, 1999). Reanalysis data at 925 hPa shows weak
625 southwesterlies (2-3 m/s) during March-April and a stronger and deeper trans-equatorial
626 southwesterly flow (6-8 m/s) during September-November (Fig. 1, side bar 1). Fig. 2 (sidebar 1)
627 shows the vertical distribution of the zonal wind at 80°W, with data from the ERA-I Renalaysis. It
628 exhibits a shallow jet during September-November and a more intense and deeper jet in September-
629 November around 5°N (Fig. 2, sidebar 1). The annual cycle of precipitation over western and
630 Andean region of Colombia is modulated by the migration of the Intertropical Convergence Zone
631 (ITCZ). The location of the ITCZ causes two wet seasons (April-May, and September-November)
632 and two dry seasons (December-February, and June-August) over central and western Colombia

(Fig. 1, sidebar 1). The second wet season (September-November) has been linked to the significant moisture transport from the Pacific Ocean through an enhanced ChocoJet (Poveda, 2004).

The Caribbean Low Level Jet (CLLJ) exhibits a pronounced annual cycle with peak winds at 925 hPa in July (14 m/s) and in January-February (10 m/s) (Amador, 2008). The enhanced jet in July has been related to seasonal variability of the North Atlantic subtropical high (Romero-Centeno et al., 2007). The jet weakens from September to November associated with relatively weak trade winds, reduced vertical wind shear, increased hurricane activity and peak precipitation over Central America (Amador, 2008). In late November when trade winds increase again, CLLJ strengthens and it reaches a maxima in February linked to increased heating over northern South America (Vizy and Cook, 2010). The vertical distribution of CLLJ shows an extension of the jet upward to 700 hPa in boreal summer, while the jet reaches up to 850 during boreal winter. The displacement of the CLLJ in the east Pacific by the ChocoJet in the boreal autumn is associated with strong precipitation over the study region (Poveda and Mesa, 2000). This displacement is modulated by El Niño/La Niña, with the latter resulting in an enhanced ChocoJet and even stronger rainfall, as, for example, in the La Niña of 2010-2011 (Arias et al., 2015).

Sidebar 2: Capacity Building

Historically, the far eastern Pacific have lacked upper-air observations. Previous attempts to perform upper-air soundings in the region failed because of difficult access to the area as a result of complex terrain and weather, safety and security issues, and lack of inter-institutional cooperation to overcome these challenges. The collaborative CHOCO-JEX program was made possible by funding of COLCIENCIAS and in-kind support of the participating institutions during the field campaigns over maritime as well as remote and difficult-to-access lands. The Universidad Nacional de Colombia at Medellín, which makes part of the largest public university in Colombia, was the leading institution in charge of the project's scientific, financial, and logistic components. During the field campaigns, FAC's in-kind support consisted of flying personnel and equipment between from Medellín to the facilities of the Center of Oceanographic and Hydrographic Research of the Pacific (DIMAR's Pacific research branch), and between Medellín and Quibdó. DIMAR facilitated the coordination and provided resources for one of the graduate students to be part of the ERFEN (Regional Study of the El Niño Southern Oscillation, in Spanish) campaigns. DRI collaborated in all stages of the project development and execution, provided expertise in atmospheric sciences and field campaigns, and contributed with in-kind support consisting in high-performance computing and analytical resources to complete the modeling component of this project (not described here). This networking among Colombian public institutions and an international research institute was one of CHOCO-JEX biggest goals and achievements.

Furthermore, the inter-institutional network created by CHOCO-JEX extended to additional activities such as the exchange of knowledge with other research groups and additional field campaigns. For example, the infrastructure and connection acquired during CHOCO-JEX enable us to participate in SeaFlower-2016, a Colombian scientific expedition in Cayo Serrana, a remote

Caribbean islet that makes part of the Colombian archipelago of San Andrés and Providencia (SeaFlower Biosphere Reserve declared by UNESCO in 2000). SeaFlower-2016 was a trans-disciplinary field campaign to study this remote region, which is affected by CLLJ. We collected atmospheric profiles during this field campaign to study the airflow-sea interaction in the region and to help understand the synoptic conditions during the observation period.

686

687 **Table 1. Description of the four IOPs during 2016 (see Fig. 1).**

IOP	Date	Region	Number of 6-hourly radiosondes launched
1	January 15-22	Oceanic	23
2	June 25 - July 1	Inland - Quibdó	25
3	October 15-21	Inland - Quibdó	28
4	November 21-28	Oceanic	30

688

689

690

691

692 **FIGURE CAPTION LIST**

693

694 **Fig. 1.** CHOCO-JEX region of interest and IOP locations. Black lines show ARC Gorgona vessel track
695 during IOP1 (red dots) and IOP4 (brown) with each dot indicating individual sounding launch position.
696 Inland soundings (IOPs 2 and 3, see text for description) were launched from Quibdó (43 m ASL) (blue
697 point). Location and name of the regional operational soundings (in purple) are also shown, including the
698 average number of soundings per year released during the period 2012–2016. Malpelo island (4.0061° N,
699 81.5936° W) is indicated as a strategic location for future oceanic campaigns.

700 **Fig. 2.** Selected pictures of CHOCO-JEX activities: (a) launching of a radiosonde from ARC Gorgona in
701 January, (b) shipping of personnel and Helium gas cylinders by Colombian Air Force in October, (c)
702 inflation of a balloon inland in Quibdó at Universidad Tecnológica del Chocó in June, and (d) sounding
703 setup on board the ARC Gorgona in November.

704 **Fig. 3.** 925 hPa average winds (vectors) and wind speed anomalies (filled contours; relative to 1980-2016)
705 during (a) January, 2016 and (b) November, 2016. Circles represent the regional low-level jets identified
706 during IOP1 and IOP4: Caribbean Low Level Jet (CLLJ), Papagayo Jet, Tehuantepec Jet, Panama Jet,
707 Llanos Jet and South American Low Level Jet (SALLJ) and Choco Low Level Jet (ChocoJet)

708 **Fig. 4.** (a) Time-longitude diagram of zonal moisture flux (g/kg*m/s) from observations and (b) averaged
709 zonal wind profiles (m/s) and specific humidity profiles from observations (black line), Era-I (red line) and
710 MERRA (blue line) during IOP1. (d) and (c) show the same as (a) and (b), respectively, but during IOP2.
711 Date thick marks indicate 00:00 UTC (19:00LST). The top x-axis during the oceanic campaign indicate the
712 distance (m) of the particular sounding relative to the coast.

713 **Fig. 5.** Same as Fig. 5 but for IOPs 3 and 4.

Fig. 6. Vertically integrated water vapor (mm; filled contours), streamlines at 850 hPa, and infrared images from GridSat-GOES (light green shades are indicative of rainfall from TRMM3B42) during IOP4. Hurricane Otto is observed in November 21 and 23 over 81°W and 10°N. Long-lasting MCSs developed around 78°W, 7°N on November 25 and 27. ARC Gorgona position over the EPAC is indicated by the white dots.

Fig. 7. Schematics of the late afternoon flow (Taken from Lopez and Howell, 1967)

Fig. 8. Diurnal cycle of observed zonal wind averages (m/s) during (a) IOP1 (January 2016; on ocean), (b) IOP2 (June, 2016; inland), (c) IOP3 (October, 2016; inland) and (d) IOP4 (November, 2016; right bottom panel). Local times relative to Colombia UTC-5.

Fig. 9. Diurnal cycle of potential temperature (Θ) anomalies (K) during IOP1 (January, 2016 on ocean), IOP2 (June, 2016 inland), IOP3 (October, 2016 inland) and IOP4 (November, 2016 on ocean).

Fig. 1 (Side bar 1). 925 hPa long-term mean (1980-2016) wind vectors and precipitation (shaded contours; mm/day) based on ERA-Interim reanalysis averaged during (a) December-February, (b) March-May, (c) June-August and (d) September-November.

Fig. 2 (Side bar 1). Vertical distribution of mean (1980-2016) zonal winds (m/s) based on ERA-Interim reanalysis at 80°W during (a) December-February, (b) March-May, (c) June-August and (d) September-November.

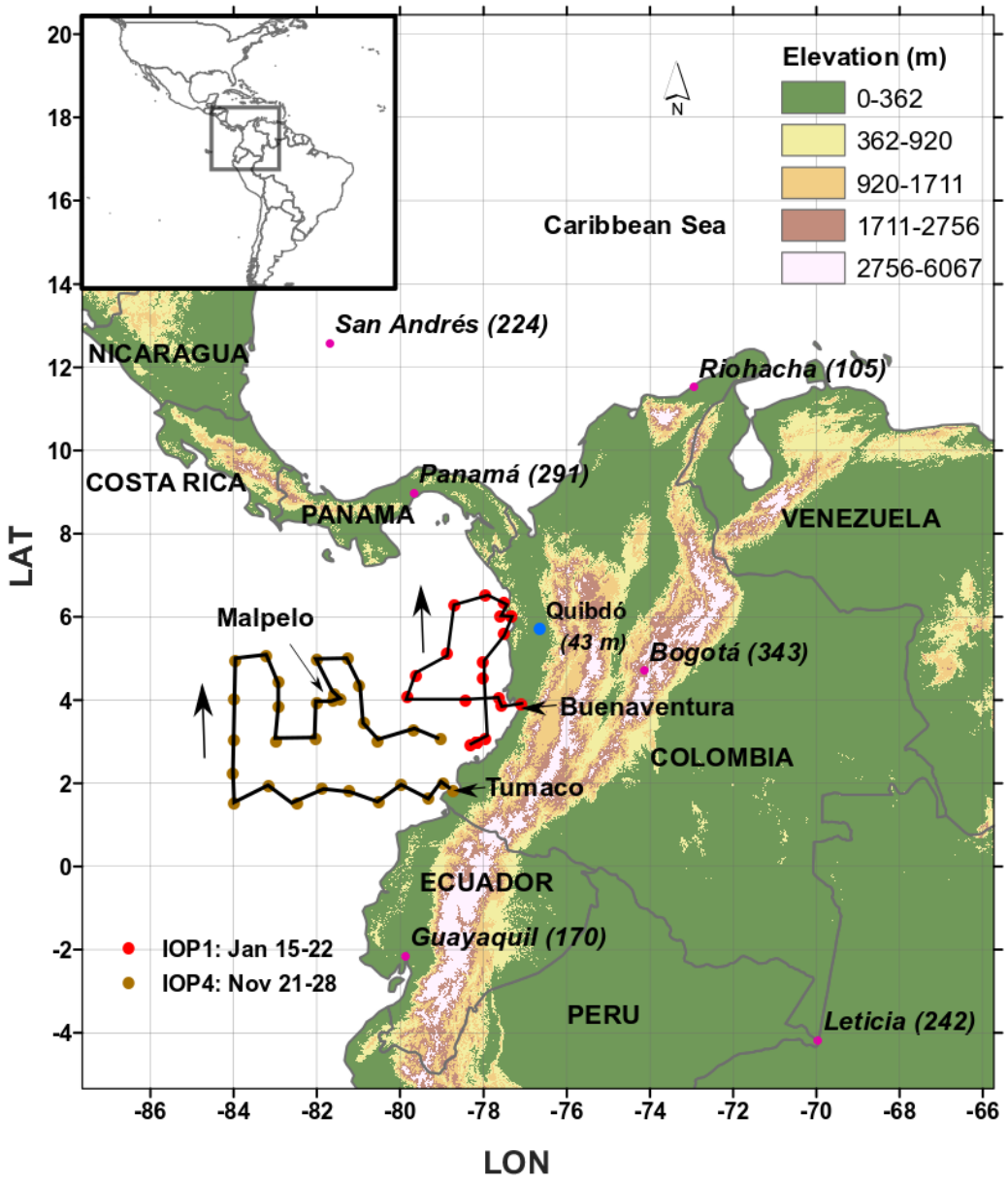

732

733 **Fig. 1.** CHOCO-JEX region of interest and IOP locations. Black lines show ARC Gorgona vessel track during IOP1 (red dots) and
734 IOP4 (brown) with each dot indicating individual sounding launch position. Inland soundings (IOPs 2 and 3, see text for description)
735 were launched from Quibdó (43 m ASL) (blue point). Location and name of the regional operational soundings (in purple) are also
736 shown (Panama, Guayaquil, Leticia, Bogotá and Riohacha) including the average number of soundings per year released during the
737 period 2012–2016. Malpelo island (4.0061° N, 81.5936° W) is indicated as a strategic location for future oceanic campaigns.

738

739

740 **Fig. 2.** Selected pictures of CHOCO-JEX activities: (a) launching of a radiosonde from ARC Gorgona in January, (b) shipping of
741 personnel and Helium gas cylinders by Colombian Air Force in October, (c) inflation of a balloon inland in Quibdó at
742 Universidad Tecnológica del Chocó in June, and (d) sounding setup on board the ARC Gorgona in November.

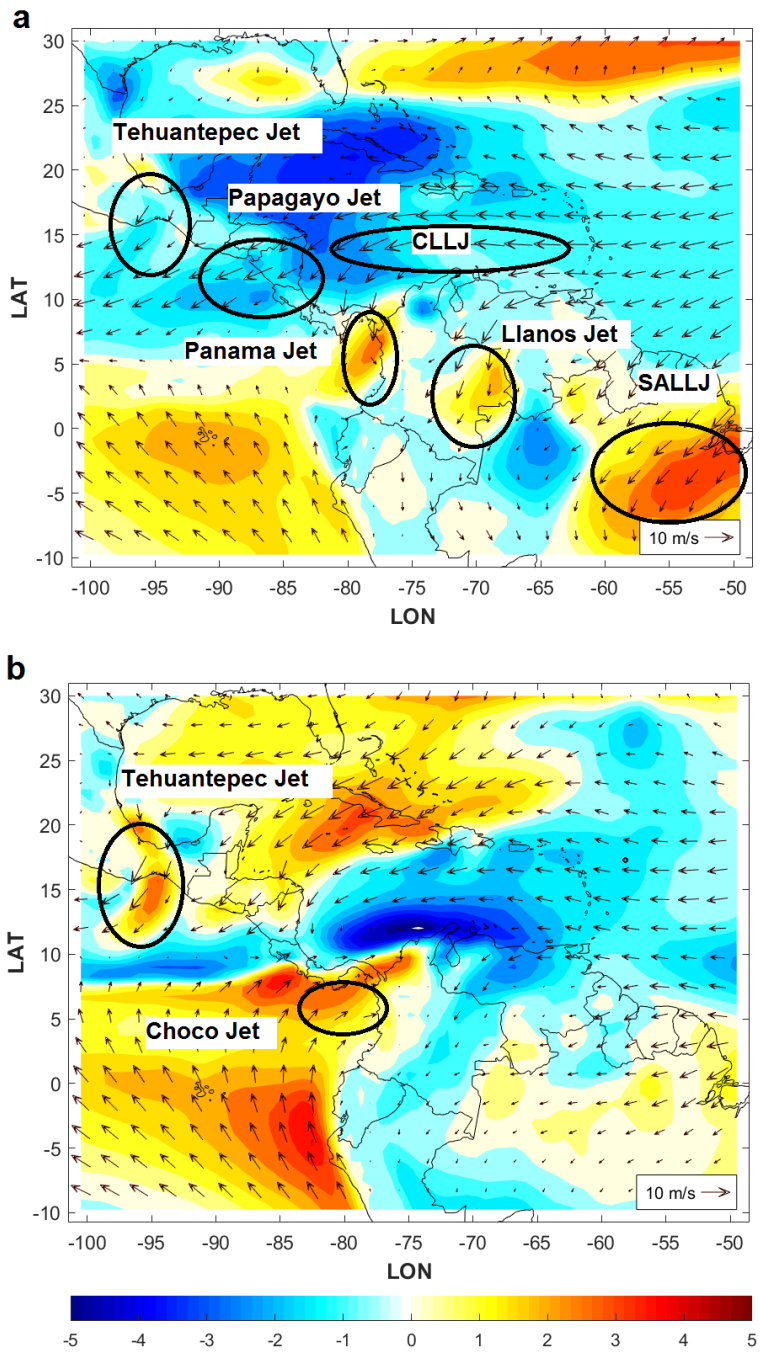

743

744 **Fig. 3.** 925 hPa average winds (vectors) and wind speed anomalies (filled contours; relative to 1980-2016) during (a) January,
745 2016 and (b) November, 2016. Circles represent the regional low level jets identified during IOP1 and IOP4: Caribbean Low
746 Level Jet (CLLJ), Papagayo Jet, Tehuantepec Jet, Panama Jet, Llanos Jet and South American Low Level Jet (SALLJ) and Choco
747 Low Level Jet (ChocoJet)

748
749

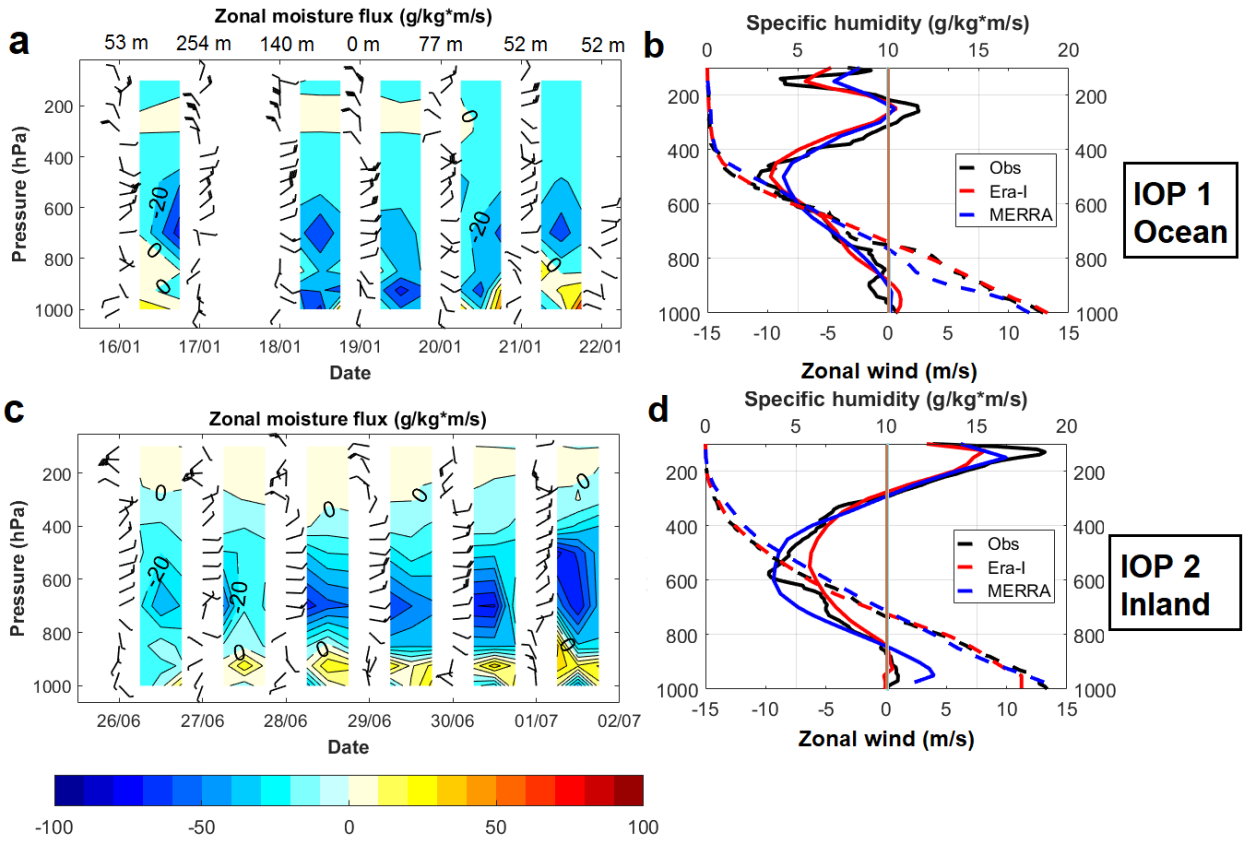

Fig. 4 (a) Time-longitude diagram of zonal moisture flux from observations (g/kg*m/s) and (b) averaged zonal wind profiles (m/s) and specific humidity profiles from observations (black line), Era-I (red line) and MERRA (blue line) during IOP1. (d) and (c) show the same as (a) and (b), respectively, but during IOP2. Date thick marks indicate 00:00 UTC (19:00LST). The top x-axis during the oceanic campaign indicate the distance (m) of the particular sounding relative to the coast.

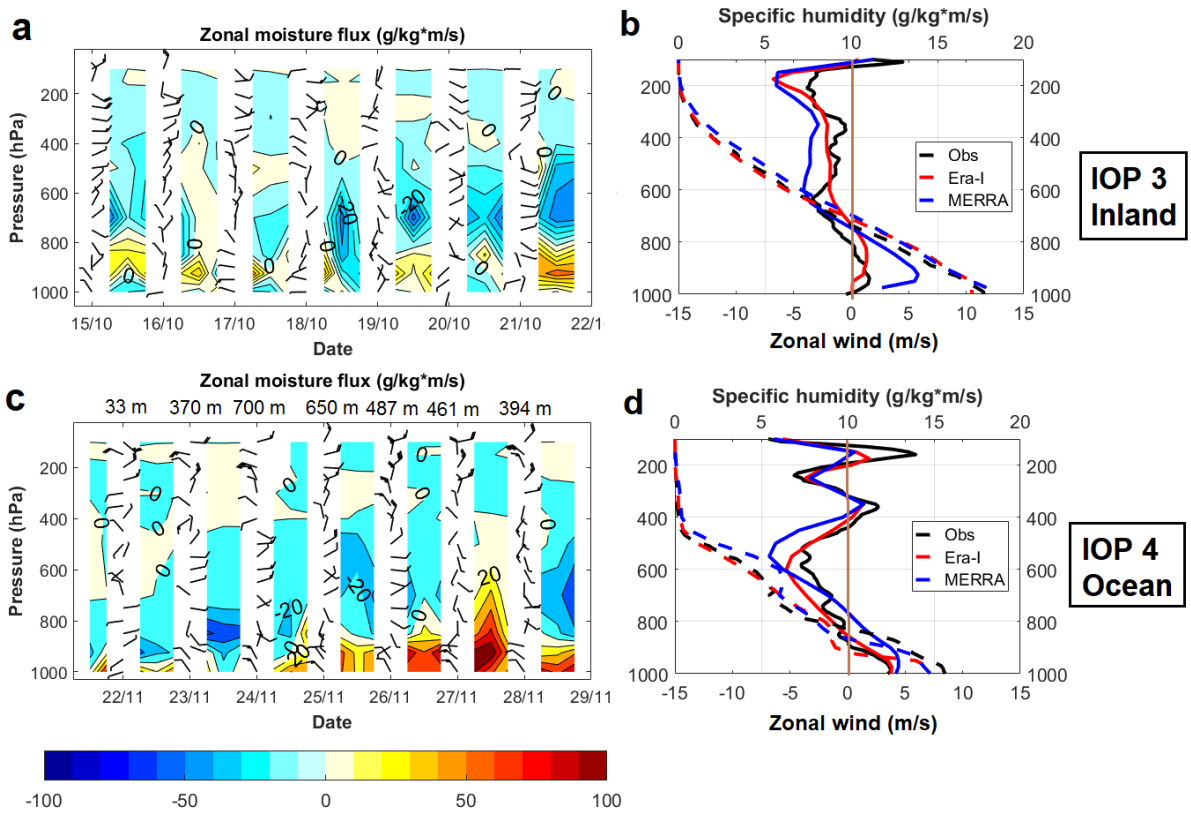

Fig. 5. Same as Fig. 5 but for IOPs 3 and 4.

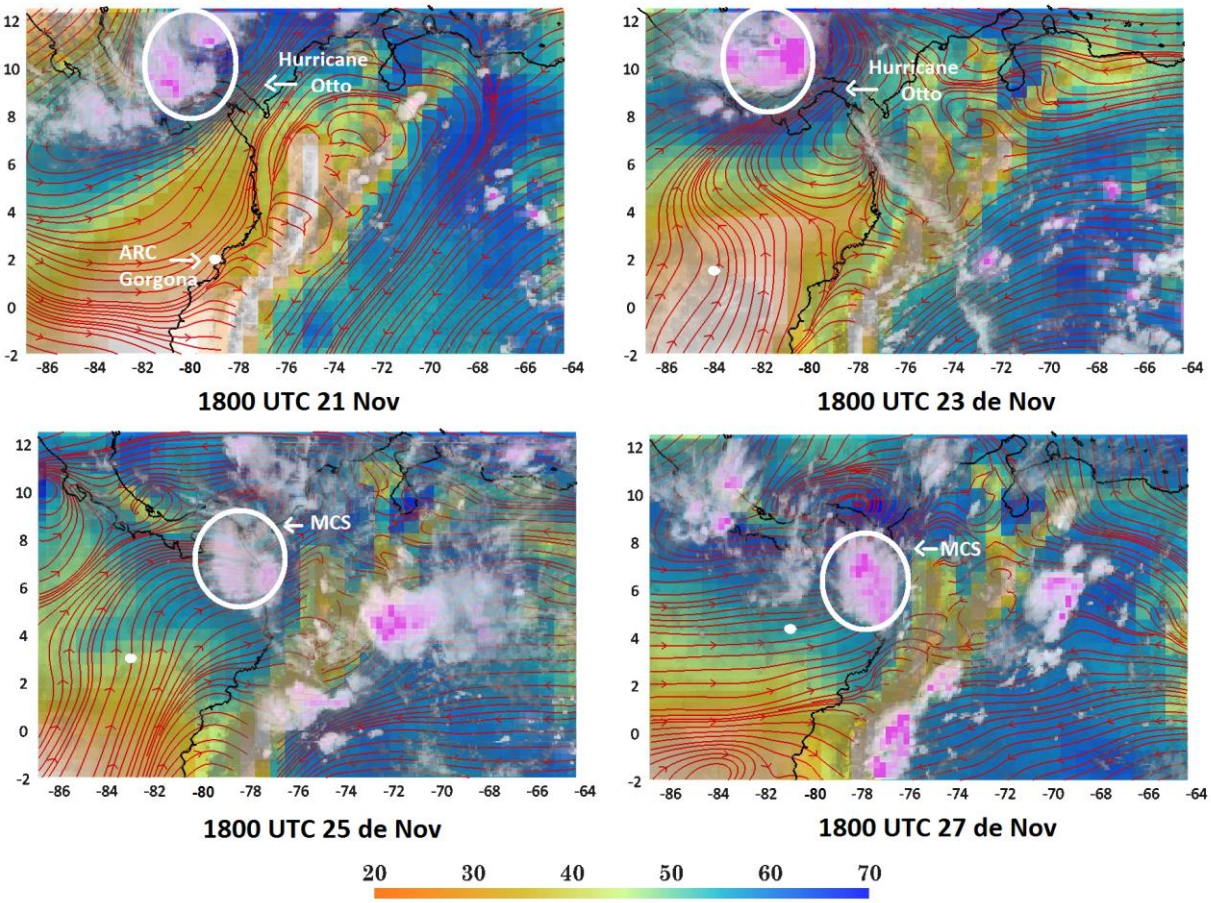

Fig. 6. Vertically integrated water vapor (mm; filled contours) and streamlines at 850 hPa from MERRA2, and infrared images from GridSat-GOES (light green shades are indicative of rainfall from TRMM3B42) during IOP4. Hurricane Otto is observed in November 21 and 23 over 81°W and 10°N. Long-lasting MCSs developed around 78°W, 7°N on November 25 and 27. ARC Gorgona position over the EPAC is indicated by the white dots.

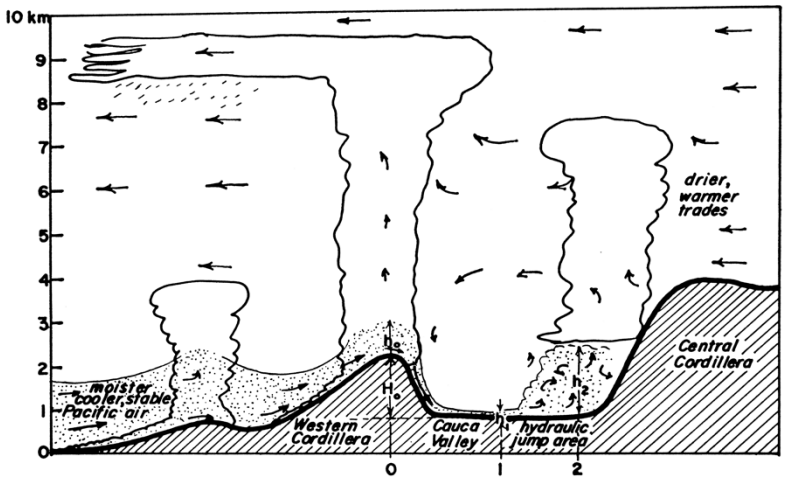

768

769 Fig. 7. Schematics of the late afternoon flow (Taken from Lopez and Howell, 1967)

770

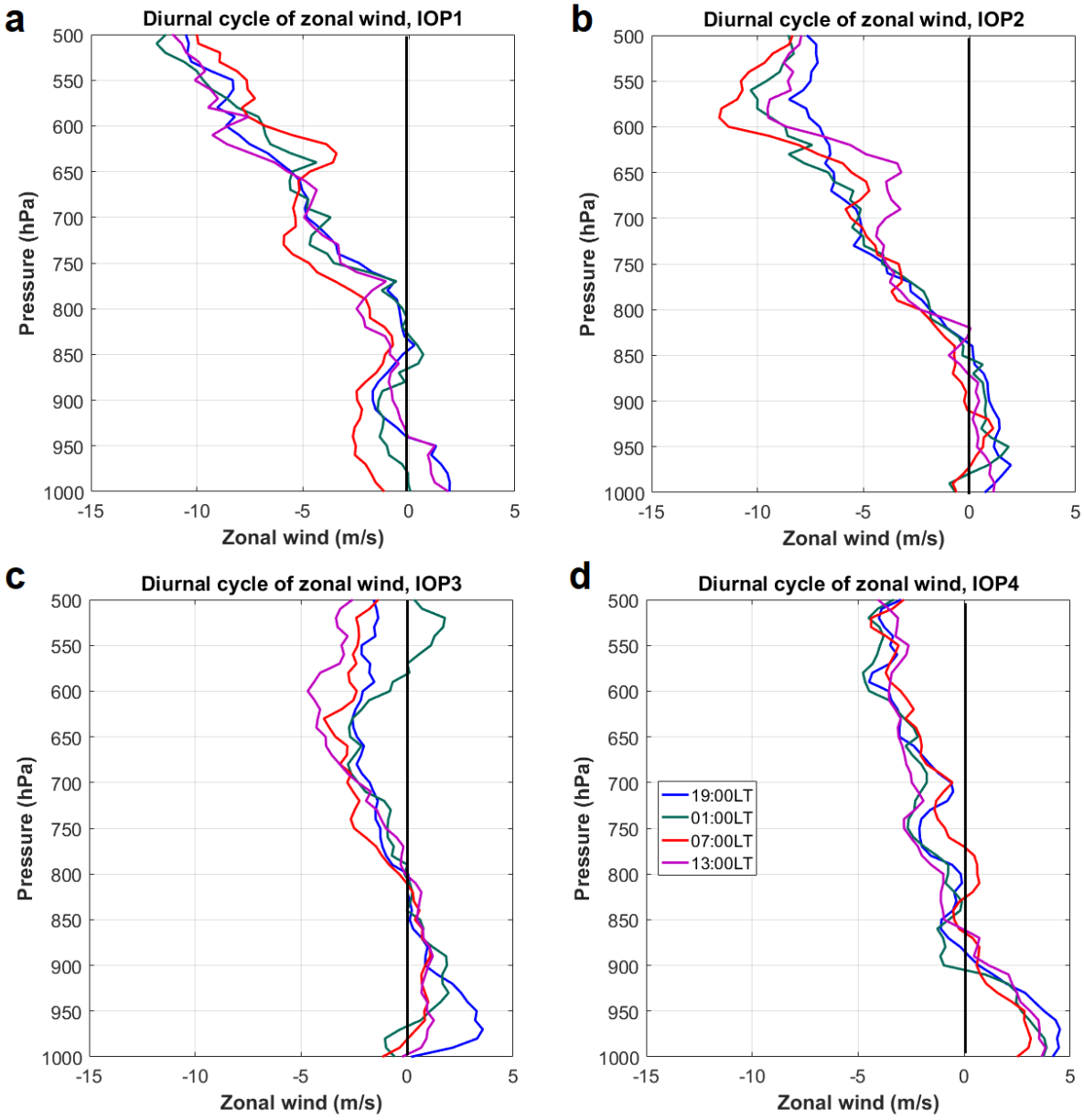

Fig. 8. Diurnal cycle of observed zonal wind averages (m/s) during (a) IOP1 (January 2016; on ocean), (b) IOP2 (June, 2016; inland), (c) IOP3 (October, 2016; inland) and (d) IOP4 (November, 2016; on ocean). Local times relative to Colombia UTC-5.

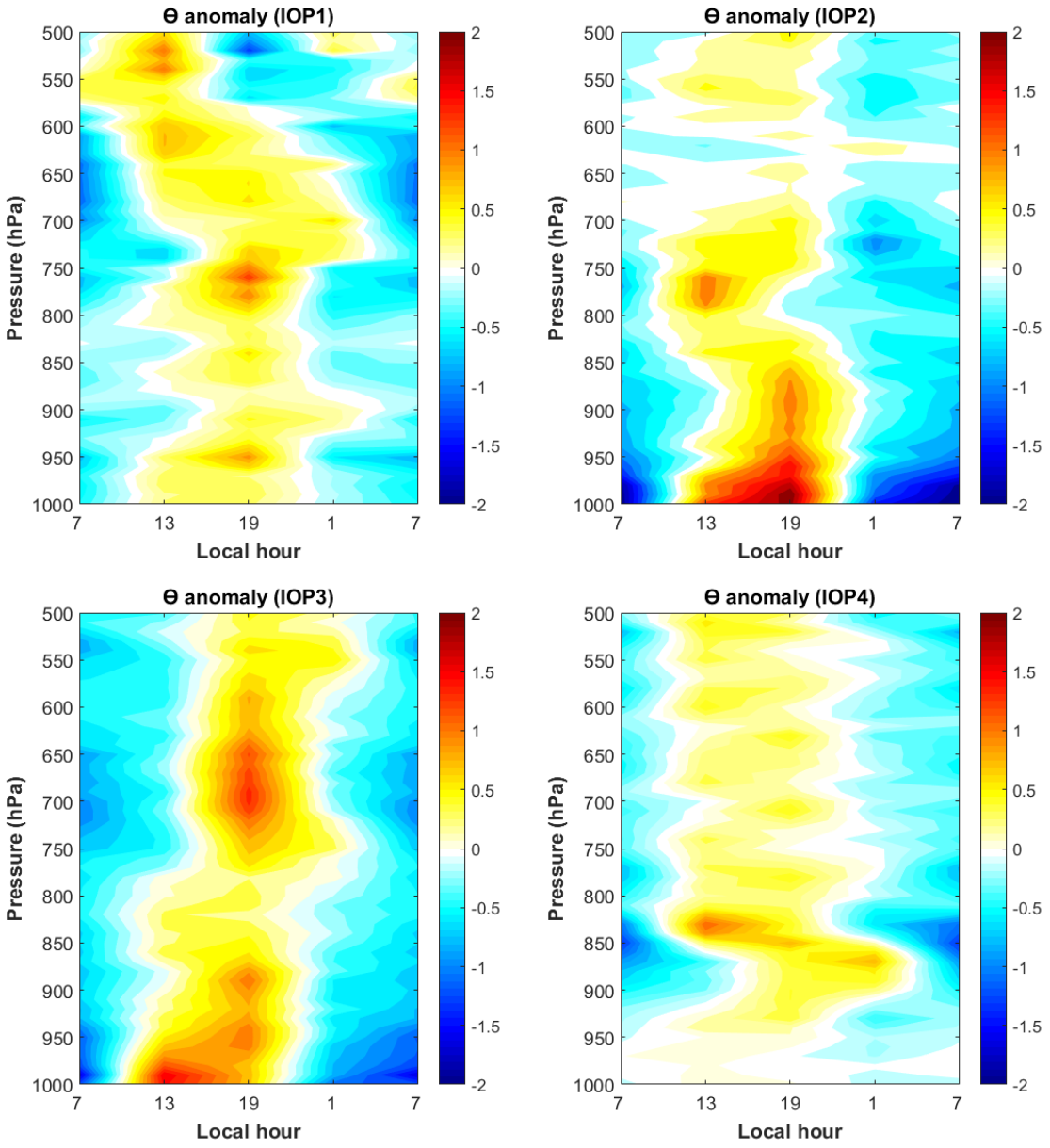

777

778

779 **Fig. 9.** Diurnal cycle of potential temperature (Θ) anomalies (K) during IOP1 (January, 2016; on ocean), IOP2 (June, 2016;
780 inland), IOP3 (October, 2016; inland) and IOP4 (November, 2016; on ocean). Local times relative to Colombia UTC-5.

781

782

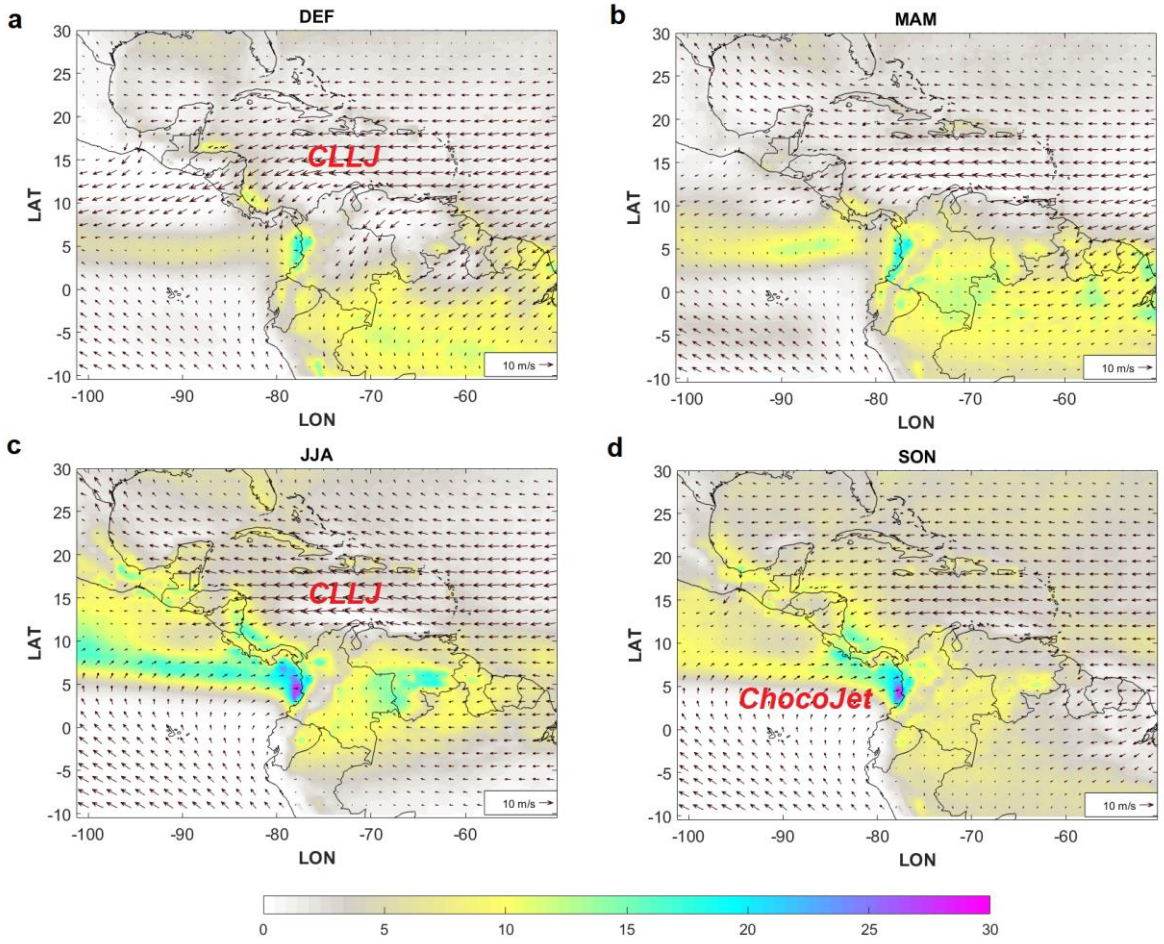

Fig. 1 (Side bar 1). 925 hPa long-term mean (1980-2016) wind vectors and precipitation (shaded contours; mm/day) based on ERA-Interim reanalysis averaged during (a) December-February, (b) March-May, (c) June-August and (d) September-November.

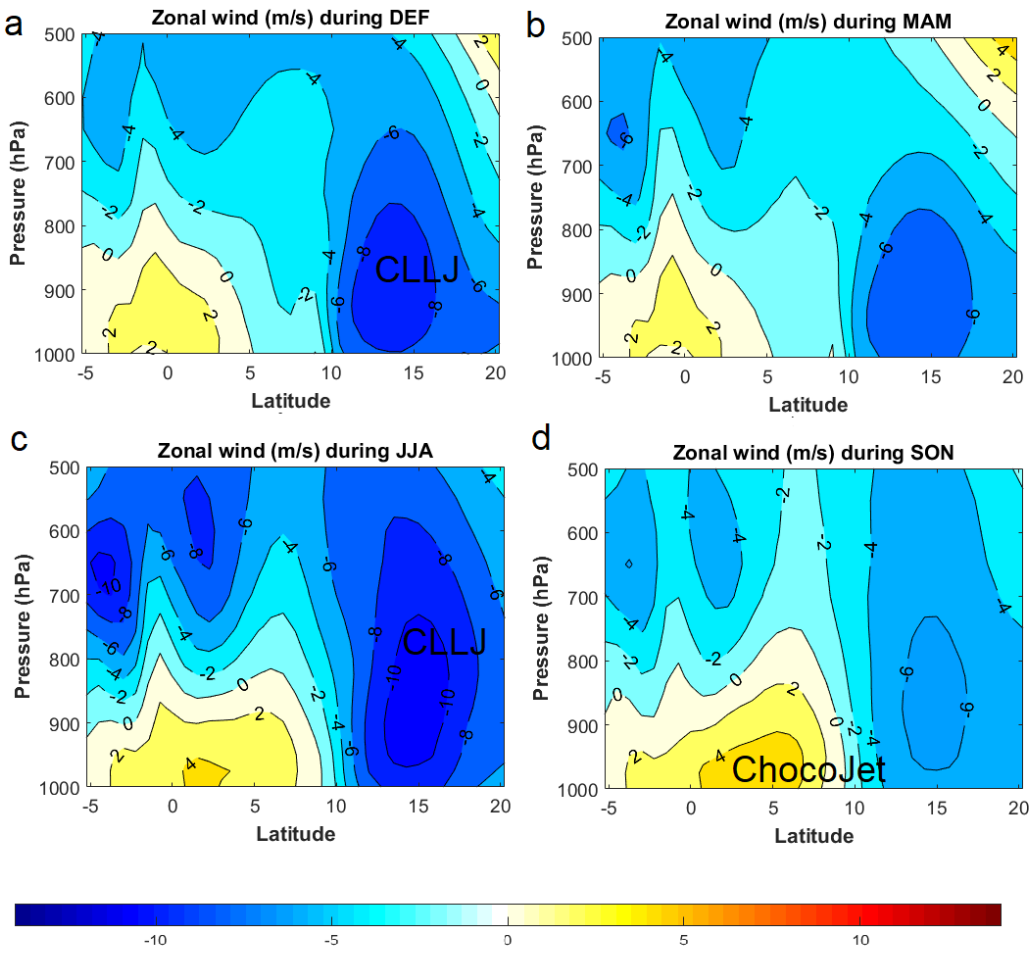

786

787 **Fig. 2 (Side bar 1).** Vertical distribution of mean (1980-2016) zonal winds (m/s) based on ERA-Interim reanalysis at 80°W
788 during (a) December-February, (b) March-May, (c) June-August and (d) September-November.

789